Neurobiology of Disease

RGS9–2 Negatively Modulates L-3,4-Dihydroxyphenylalanine-Induced Dyskinesia in Experimental Parkinson's Disease

Stephen J. Gold,[1] Chau V. Hoang,[1] Bryan W. Potts,[1] Gregory Porras,[2] Elsa Pioli,[2] Ki Woo Kim,[1] Agnes Nadjar,[2] Chuan Qin,[3] Gerald J. LaHoste,[4] Qin Li,[3] Bernard H. Bioulac,[2] Jeffrey L. Waugh,[1] Eugenia Gurevich,[5] Rachael L. Neve,[6] and Erwan Bezard[2,3]

[1]Department of Psychiatry, University of Texas Southwestern Medical Center at Dallas, Dallas, Texas 75390, [2]Centre National de la Recherche Scientifique, Unité Mixte de Recherche 5227, Universite Victor Segalen-Bordeaux 2, 33076 Bordeaux, France, [3]Institute of Lab Animal Sciences, Chinese Academy of Medical Sciences, 100021 Beijing, China, [4]Department of Psychology, University of New Orleans, New Orleans, Louisiana 70148, [5]Department of Pharmacology, Vanderbilt University Medical Center, Nashville, Tennessee 37232, and [6]Department of Genetics, Harvard Medical School, Belmont, Massachusetts 02478

Chronic L-dopa treatment of Parkinson's disease (PD) often leads to debilitating involuntary movements, termed L-dopa-induced dyskinesia (LID), mediated by dopamine (DA) receptors. RGS9–2 is a GTPase accelerating protein that inhibits DA D2 receptor-activated G proteins. Herein, we assess the functional role of RGS9–2 on LID. In monkeys, Western blot analysis of striatal extracts shows that RGS9–2 levels are not altered by MPTP-induced DA denervation and/or chronic L-dopa administration. In MPTP monkeys with LID, striatal RGS9–2 overexpression – achieved by viral vector injection into the striatum – diminishes the involuntary movement intensity without lessening the anti-parkinsonian effects of the D1/D2 receptor agonist L-dopa. In contrasts, in these animals, striatal RGS9–2 overexpression diminishes both the involuntary movement intensity and the anti-parkinsonian effects of the D2/D3 receptor agonist ropinirole. In unilaterally 6-OHDA-lesioned rats with LID, we show that the time course of viral vector-mediated striatal RGS9–2 overexpression parallels the time course of improvement of L-dopa-induced involuntary movements. We also find that unilateral 6-OHDA-lesioned RGS9$^{-/-}$ mice are more susceptible to L-dopa-induced involuntary movements than unilateral 6-OHDA-lesioned RGS9$^{+/+}$ mice, albeit the rotational behavior – taken as an index of the anti-parkinsonian response – is similar between the two groups of mice. Together, these findings suggest that RGS9–2 plays a pivotal role in LID pathophysiology. However, the findings also suggest that increasing RGS9–2 expression and/or function in PD patients may only be a suitable therapeutic strategy to control involuntary movements induced by nonselective DA agonist such as L-dopa.

Key words: **RGS proteins; dopamine receptor; Parkinson's disease; knock-out mouse; dyskinesia; monkey**

Introduction

Chronic dopamine (DA) replacement therapy with L-3,4-dihydroxyphenylalanine (L-dopa) in Parkinson's disease (PD) results in motor complications known as L-dopa-induced dyskinesia (LID) in up to 80% of patients within 5 years of treatment (Rascol et al., 2000). The G-protein-coupled DA receptors (DAR) are expressed by striatal medium spiny neurons (MSNs) connecting the striatum to the basal ganglia output nuclei through the so-called "direct" and "indirect" pathways (Alexander and Crutcher, 1990) (but see Nadjar et al., 2006). The GABAergic direct pathway projects directly to the internal segment of the globus pallidus (GPi) and expresses the D1 DA receptor (D1R), whereas the GABAergic indirect pathway, directed at the external pallidal segment (GPe), expresses the D2 DA receptor (D2R). DA is supposed to activate the direct pathway through D1R and to inhibit the indirect pathway through D2R. In PD, loss of DA creates an imbalance between the two pathways leading to a braking hyperactivity of the output structures of the basal ganglia, whereas LID are thought to result from both an excessive activation of the D1R-expressing striato-GPi pathway activity and an excessive inhibition of the D2R striato-GPe projection (Cenci, 2007).

Although numerous data support the involvement of an increased D1R signaling in LID (Cenci et al., 1998; Picconi et al., 2003; Aubert et al., 2005), the impact of the excessive inhibition of the striato-GPe projection through D2R overactivity remains to be elucidated. Because dampening such D2R-mediated signaling could theoretically decrease LID intensity, we focused on the

Received March 26, 2007; accepted Nov. 11, 2007.

This work was supported by National Alliance for Research on Schizophrenia and Depression Young Investigator Award (S.J.G.), an American Heart Association Texas Affiliate Beginning Grant-in-Aid (S.J.G.), National Institute on Drug Abuse Grant PO1 DA 008227-12 (S.J.G.), National Institute of Mental Health Grant P50 MH66172 (S.J.G.), Michael J. Fox Foundation for Parkinson Research (E.B.), and Fondation de France (E.B.). We are grateful for the excellent technical assistance of Anita Autry, Joshua Lerman, and Joshua Schonborn.

Correspondence should be addressed to Erwan Bezard, Centre National de la Recherche Scientifique, Unité Mixte de Recherche 5227, Universite Bordeaux 2, 146 Rue Leo Saignat, Bordeaux 33076, France. E-mail: erwan.bezard@u-bordeaux2.fr.

S. J. Gold's present address: Merck Research Laboratories, Rahway, NJ 07065.

DOI:10.1523/JNEUROSCI.4223-07.2007

 0270-6474/07/2714338-11$15.00/0

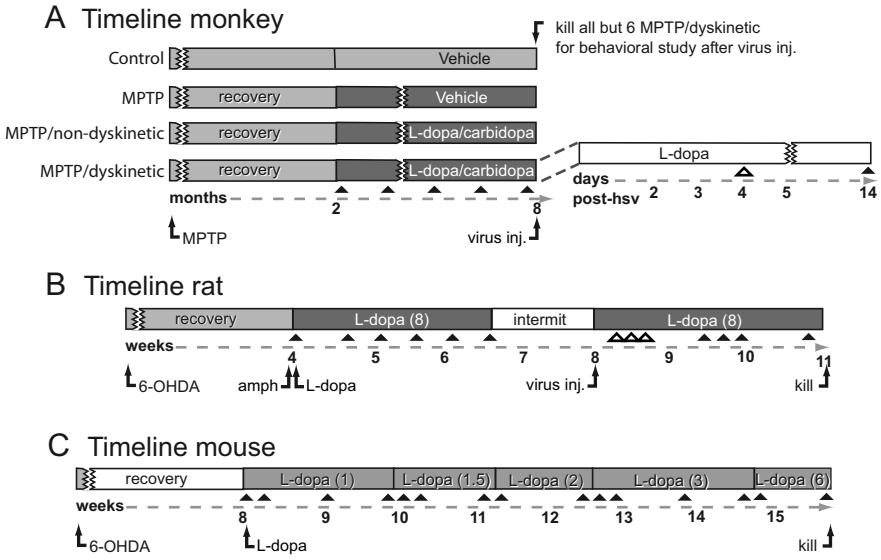

Figure 1. Schematized timelines for primate and rodent behavioral experiments. ***A***, Timeline for monkey experiments showing sequence of events, including MPTP intoxication, chronic L-dopa treatment, intracranial virus injection, and postviral monitoring. In ***A–C***, (1) LID/AIM observations are indicated by upward pointing arrowheads below line, (2) open arrowheads indicate observations occurring during maximal viral-mediated overexpression, (3) numbers in parentheses are dose of L-dopa (mg/kg), (4) unless otherwise indicated, numbers under dashed line are weeks or months after lesion. Parkinsonian disability in the monkey study (***A***) was assessed on the same day as dyskinesia score. ***B***, Timeline for rat experiments showing sequence of events, including unilateral 6-OHDA lesion, recovery period, amphetamine challenge, initiation of daily L-dopa injections (8 mg/kg), period of every other day injections (intermit), and intracranial virus injection and kill. ***C***, Timeline for mouse experiments showing sequence of events, including unilateral 6-OHDA lesion, recovery period, and initiation of daily L-dopa injections and kill.

D2R-signaling cascade and its regulation. The regulators of *G*-protein *s*ignaling (RGS) family of proteins (Berman and Gilman, 1998; Ross and Wilkie, 2000) negatively modulate G-protein-coupled receptor (GPCR) signaling via their GTPase accelerating protein (GAP) activity at G α subunits. Among the numerous RGS genes expressed in the brain (Gold et al., 1997), the RGS9–2 splice variant is highly enriched in striatal MSNs (Granneman et al., 1998; Rahman et al., 1999). RGS9–2 knock-out mice show heightened locomotor responses to dopaminergic drugs in both normal (Rahman et al., 2003) and DA-depleted rodents (Kovoor et al., 2005). Conversely, viral-mediated overexpression of RGS9–2 reduced locomotor responses to D2R, but not D1R agonists (Rahman et al., 2003).

Because these data strongly suggested that experimentally enhanced RGS9–2 activity could decrease the intensity of LID, we tested whether transient herpes simplex virus (HSV)-mediated RGS9–2 expression could dampen LID severity in the macaque model of PD and LID without interfering with the therapeutic action of anti-parkinsonian DAergic drugs. We further validated the time course of transient viral-mediated expression in the unilateral 6-hydroxydopamine (6-OHDA) rat model of AIMs and tested the converse hypothesis, that lack of RGS9–2 would increase expression of LID in the unilateral 6-OHDA mouse model of AIMs using RGS9–2 knock-out mice. Our results support our hypothesis that increased RGS9–2 activity decreases LID severity in the gold standard primate model of LID. However, this diminished LID is at the cost of the anti-parkinsonian effect when using a specific D2R agonist, suggesting the approach could only be used in combination with L-dopa.

Materials and Methods

All experiments were performed in accordance with both the European Communities Council Directive of November 24, 1986 (86/609/EEC) for the care of laboratory animals and the Institutional Animal Care and Use Committee of University of Texas Southwestern Medical Center in Association for Assessment and Accreditation of Laboratory Animal Care International accredited facilities.

Monkey studies

Housing. We used 22 female cynomolgus monkeys (*Macaca fascicularis*; SAH/Xierxin, Beijing, People's Republic of China). Animals were housed in individual primate cages under controlled conditions of humidity, temperature, and light (12 h light/dark cycle, lights on at 8:00 A.M.); food and water were available *ad libitum*. Animal care was supervised by veterinarians skilled in the healthcare and maintenance of nonhuman primates.

Experimental parkinsonism and dyskinesia. Experiments were conducted according to previously published procedures and methods (Bezard et al., 2003; Aubert et al., 2005; Guigoni et al., 2005b). Eighteen monkeys received once daily intravenous injections of 1-methyl-4-phenyl 1,2,3,6-tetrahydropyridine (MPTP) hydrochloride (0.2 mg/kg) until they displayed parkinsonian symptoms (mean number of injections, 15 ± 1) (Bezard et al., 2001), whereas four received vehicle only (Fig. 1*A*, Table 1). It took an average of 8 weeks for the bilateral parkinsonian syndrome to stabilize (i.e., constant disability score over 2 consecutive weeks). Among the 18 MPTP-treated monkeys, four monkeys were kept without any dopaminergic supplementation but received vehicle (MPTP/vehicle group: "parkinsonian"), whereas 14 were treated chronically with twice-daily administration of Modopar (L-dopa/carbidopa, ratio 4:1; Roche, Basel, Switzerland) for 6 months at a tailored dose designed to fully reverse the parkinsonian features (Fig. 1*A*, Table 1). Ten of these 14 monkeys developed dyskinesia (MPTP/dyskinetic group: "parkinsonian dyskinetic"), whereas four did not (MPTP/nondyskinetic group: "parkinsonian nondyskinetic") (Fig. 1*A*, Table 1).

All monkeys, but 6 MPTP/dyskinetic that were kept alive for additional behavioral experiments (see below) (Fig. 1*A*), were killed by sodium pentobarbital overdose (150 mg/kg, i.v.) 1 h after the last vehicle or L-dopa/carbidopa dose. Brains were removed quickly and divided into the two hemispheres. The right hemisphere was immediately frozen by immersion in isopentane and then stored at −80°C. The left hemisphere was dissected for isolating the striatum (combining caudate nucleus, putamen and nucleus accumbens, across the rostrocaudal extent) that was then frozen in isopentane and stored at −80°C (Nadjar et al., 2006).

Assessment of lesion. DA transporter binding using [^{125}I]-(E)-N-(3-iodoprop-2-enyl)-2β-carboxymethyl-3β-(4′-methylphenyl)-nortropane (PE2I; Chelatec, Nantes, France) was measured as previously described (Bezard et al., 2001; Guigoni et al., 2005a). Processing of mesencephalic sections for tyrosine hydroxylase (TH) immunohistochemistry, counterstaining with cresyl violet (Nissl staining) and cell counts (Visioscan version 4.12; Biocom, Les Ulis, France) were performed as described previously (Bezard et al., 2001; Guigoni et al., 2005a). The boundaries of the SNc were chosen on three consecutive sections corresponding to a representative median plane of the SNc by examining the size and shape of the different TH-immunoreactive neuronal groups, cellular relationships to axonal projections and nearby fiber bundles. The number of both TH-immunoreactive and Nissl-stained neurons per SNc representative plane was calculated three times by one examiner blind with regard to the experimental condition. Split cell counting error was corrected by using the formula of Abercrombie (1946). Mean cell number per plane and SEM were then calculated for each group of monkey.

Western blot analysis. Western blot analysis was performed as previously described (Gold et al., 2003; Krumins et al., 2004) using the following primary antibodies: rabbit antiserum against the C terminus of RGS2

(CKKPQITTEPHAT; 1:1000; a generous gift from D. Siderovski, University of North Carolina, Chapel Hill, NC); rabbit antisera against rat RGS4 (Krumins et al., 2004) (1:2000; a generous gift from S. Mumby, University of Texas Southwestern Medical Center, Dallas, TX), affinity purified anti-RGS7 antibodies (Upstate Biotechnologies; 1:10,000), protein A-purified rabbit antibodies made in our laboratory to his-tagged RGS9c bacterially expressed fragment (He et al., 1998), and SGS rabbit antisera against Gβ5 (Zhang et al., 1996) (1:5000; a generous gift from W. Simonds, National Institute of Diabetes and Digestive and Kidney Diseases, Bethesda, MD). The specificities of these RGS and Gβ5 antibodies were further confirmed using brain extracts from wild-type (wt) and mutant mice (supplemental Fig. 1, available at www.jneurosci.org as supplemental material) (Gβ5 data not shown). Western blot images on autoradiographic film were captured with a CCD camera (ExwaveHAD; Sony, Tokyo, Japan) and quantified densitometrically with NIH Image (version 1.61). To control for variations in lane loading, blots were re-processed for total Gβ immunoreactivity using rabbit antisera against pan-Gβ [B600; a generous gift from S. Mumby (Linder et al., 1993)]. RGS Immunoreactivity levels presented were normalized to total Gβ immunoreactivity.

Table 1. Behavioral and anatomical validation

Groups		DAT binding	Number of TH$^+$ cells	L-Dopa				
					0 min		90 min	
				mg	P	D	P	D
Control	C1	123.9	922		0	0	0	0
	C2	154.5	958		0	0	0	0
	C3	134.9	1007		0	0	0	0
	C4	144.4	935		0	0	0	0
MPTP	M1	1.6	137		9	0	0	0
	M2	3.4	140		9	0	0	0
	M3	2.7	74		8	0	0	0
	M4	3.5	198		9	0	0	0
MPTP	L1	3.9	127	54	9	0	0	0
L-Dopa :no LID	L2	2.9	237	59	11	0	0	0
	L3	4.2	169	56	9	0	0	0
	L4	5.3	134	50	8	0	0	0
MPTP	D1	5.6	217	60	9	0	1	4
L-Dopa LID	D2	7.7	106	66	8	0	0	3
	D3	0.8	155	53	7	0	0	4
	D4	4.1	178	50	8	0	0	3
MPTP	D5	3.3	132	52	9	0	1	4
L-Dopa LID	D6	3.2	177	51	10	0	0	3
HSV-LacZ	D7	4.5	159	58	11	0	1	4
MPTP	D8	1.5	107	50	11	0	1	4
L-Dopa LID	D9	2.0	141	57	10	0	0	4
HSV-RGS9–2	D10	6.4	206	61	10	0	0	3

Mean age, 3.05 ± 0.05 years; mean weight, 3.1 ± 0.1 kg. No LID, Nondyskinetic; LID, dyskinetic. Extent of lesion is comparable among the MPTP-lesioned groups at both the striatal [dopamine transporter (DAT) binding, femtomoles per milligram of equivalent tissue] and nigral [tyrosine hydroxylase (TH) immunopositive neurons] levels. L-Dopa dose (in milligrams) is given for each individual as well as their mean parkinsonian (P) and mean dyskinetic (D) scores before administration (0 min) and 90 min after administration.

Stereotactic surgery. Six MPTP/dyskinetic monkeys were used to assess whether viral-mediated RGS9–2 expression in motor striatum could attenuate LIDs. The timeline of these studies are illustrated schematically in Figure 1*A*. Because individual macaques differ greatly with regard to specific intracerebral sites, the standard Horsley-Clarke stereotaxic technique has been improved by using sagittal and frontal ventriculography (Feger et al., 1975) to locate with accuracy the borders of the third ventricles and the edges of the anterior (AC) and posterior commissures, as previously described (Bezard et al., 1999; Boraud et al., 2001). Actual position of left and right putamen is then defined by combining the ventriculography-defined position of the AC and the stereotaxic population-based historical atlas of the basal ganglia (Francois et al., 1996). Intracerebral injection of either HSV-RGS9–2 ($n = 3$) or HSV-LacZ ($n = 3$) is then performed with a 25 μl Hamilton syringe mounted into a Kopf microinjector system at five rostrocaudal levels (10 μl at each level) from AC (AC-0 mm) to 4 mm caudal to AC (AC-4 mm) 1 mm apart, 3 mm above the virtual horizontal line passing through AC and posterior commissural (see Fig. 3*H*) (total injected volume = 50 μl). After each injection, the syringe was left in place for 5 min to prevent leakage of the vector along the needle track. The Hamilton syringe was refilled between each track.

HSV behavioral experiments. Monkeys' behavioral responses to their tailored dose of L-dopa/carbidopa (ranging between 15 and 20 mg/kg for maximal reversal of PD symptoms; administration at 7:00 A.M.) and to 0.6 mg/kg of the D2/D3 agonist ropinirole (administration at 3:00 P.M.) (Rascol et al., 2000), were defined before HSV intracerebral injections. Before 3:00 P.M., i.e., before the ropinirole challenge, all animals were back to the full parkinsonian state. Monkeys recovered from surgery for 2 d. Four days post-HSV injection, animals were assayed for behavioral responses to L-dopa (A.M.) and ropinirole (P.M.). Last, on 14 d after injection, monkeys were assayed again for their behavioral responses.

Parkinsonian condition (and its reversal) was assessed on a parkinsonian monkey rating scale using videotape recordings of monkeys as previously described (Bezard et al., 2003; Guigoni et al., 2005b). A score of 0 corresponds to a normal animal and a score above 6 to a parkinsonian animal. The severity of dyskinesia was rated using the Dyskinesia Disability Scale: 0, dyskinesia absent; 1, mild, fleeting, and rare dyskinetic postures and movements; 2, moderate, more prominent abnormal movements, but not interfering significantly with normal behavior; 3, marked, frequent and, at times, continuous dyskinesia intruding on the normal repertoire of activity; or, 4, severe, virtually continuous dyskinetic activity replacing normal behavior and disabling to the animal. Locomotor activity was concomitantly monitored with infrared activity monitors, providing a mobility count every 5 min (Bezard et al., 2003).

Rat studies

6-OHDA lesion and AIM induction. Timeline of experiments is depicted on Figure 1*B*. Unilateral, 6-OHDA-lesioned, L-dopa/benserazide-treated rats were generated as described previously (Meissner et al., 2006). Male Wistar rats (Charles River, Kingston, NY) (250–350 gm) were pretreated with desipramine (25 mg/kg, i.p.) and pargyline (5 mg/kg, i.p.), anesthetized with chloral hydrate (400 mg/kg, i.p.) and then placed in a stereotaxic frame (David Kopf Instruments, Tujunga, CA). 2.5 μl of 6-OHDA.Br (5 mg/ml) was injected into the right medial forebrain bundle [anterior (A), − 4.0 mm; lateral (L), 1.1 mm; ventral (V), − 7.6 mm (Paxinos and Watson, 1986)] at a rate of 0.5 μl/min. The injection cannula was left in place for 5 more min before removal. At 4 weeks after lesion, rats were screened for lesion quality by assessing ipsilateral turns completed in 45 min after amphetamine sulfate (5 mg/kg, i.p.). A seven turns per minute minimum criteria was used to exclude rats from the assay. They were then injected intraperitoneally with L-dopa methyl-ester (8 mg/kg) and benserazide (8 mg/kg) once daily (sterile water as vehicle) and assessed for L-dopa/benserazide-induced abnormal involuntary movement (AIM) using a 0–4 AIM rating scale (Lundblad et al., 2002). Rats were observed by two blinded, trained observers for rotations and for axial, forelimb and orolingual AIMs, while concomitantly videotaping the behaviors. Observers scored each rat every 15 min. As described by Cenci et al. (2002), we found the behavioral AIM measures to be objective and reproducible, reaching inter-rater reliability measures of 87%. When AIM intensities reached an asymptote at 2.5 weeks of treatment, rats were switched to an intermittent (every other day) schedule of L-dopa/benserazide injections and continued to exhibit intense AIM.

HSV behavioral experiments. Ten days after reaching the AIM asymptote, rats were anesthetized as described above and stereotaxically in-

jected at two sites in the denervated dorsolateral striatum with 2 μl each of either HSV-LacZ ($n = 14$) or HSV-RGS9–2 ($n = 6$) (Rahman et al., 2003) at a rate of 0.5 μl/min. Stereotaxic coordinates relative to bregma and the dural surface were (in mm): target 1: anteroposterior (A/P), 0.2; mediolateral (M/L), 3.7; dorsoventral (D/V), 4.6; target 2: A/P, 0.15; M/L, 3.7; D/V, 4.6 with the bite bar set to −2.4 mm. At the expected height of transgene overexpression, 3–5 d after HSV injection (Carlezon et al., 1997; Barrot et al., 2005), animals were scored for AIM responses to L-dopa (8 mg/kg)/benserazide (8 mg/kg) and three HSV-LacZ animals were killed for X-gal staining by perfusion with 2% paraformaldehyde. Last, on 11, 13, 15, and 20 d after injection, time points when HSV-mediated transgene overexpression has ceased (Carlezon et al., 1997; Barrot et al., 2005), rats were assayed again for AIM. As control, on 13 d after injection, three HSV-LacZ animals were killed for X-gal staining by perfusion with 2% paraformaldehyde. On day 21 after HSV injection, all rats were killed by decapitation at the height of AIM, 1 h after L-dopa injection. Dorsal striatal samples from the lesioned and unlesioned hemispheres were obtained by free-hand dissection and rapidly frozen in dry ice. Lesion quality was assessed by Western blot analysis for TH levels. None of the rats showed levels of dorsal striatal TH immunoreactivity that was <95% reduced from the unlesioned side.

X-gal staining. After thorough rinsing in phosphate buffered saline (PBS), 40 μm free-floating cryostat-cut sections were incubated 12 h at 37°C in X-gal staining solution (0.1 M PBS, 1 mM potassium ferricyanide, 1 mM potassium ferrocyanide, 0.4 mM magnesium chloride, 0.02% Igepal CA-630, 0.01% Deoxycholate acid, 2% X-gal solution in DMSO). The reaction was stopped by rinsing in PBS before counterstaining with Nuclear Fast Red (Vector).

Pattern and extent of HSV-mediated RGS9–2 expression. This viral vector gives rise to a high expression of biologically active RGS9–2 protein that comigrates with endogenous RGS9–2 by SDS-PAGE (Rahman et al., 2003; Zachariou et al., 2003). Unfortunately, academically and commercially produced anti-RGS9 antibodies were not suitable for immunohistochemical localization of RGS9–2. Thus, to visualize viral-mediated RGS9–2 expression histochemically, we circumvented the antibodies issue by injecting two rats with an HSV vector expressing an N terminus Myc-tag RGS9–2 (HSV volume and stereotactic target as above). Myc immunohistochemistry was performed on tissue sections from HSV-Myc-RGS9–2 infected rats killed by transcardial perfusion 4 d after intracranial virus injection using a monoclonal antibody from Millipore (Temecula, CA) diluted 1:500 with standard avidin-biotin horseradish peroxidase procedures and DAB as chromogen.

Mouse studies

6-OHDA lesion and AIM induction. The temporal sequence of the mouse experiments are illustrated schematically in Figure 1*C*. The RGS9$^{-/-}$ line of mice was described previously (Chen et al., 2000). Male and female wt and RGS9$^{-/-}$ mice were propagated via RGS9$^{+/-}$ × RGS9$^{+/-}$ breeding and assigned to groups with a goal of littermate comparisons. Unilateral 6-OHDA MFB lesions were performed on male and female mice with minor modifications as described by Lundblad et al. (2004). Mice were anesthetized with ketamine hydrochloride (100 mg/kg)/xylazine (9 mg/kg) mixture and injected with desipramine (2.5 mg/kg) 30 min before infusion of 6OHDA, placed on a heating pad in a stereotaxic apparatus and then 1 μl of 6-OHDA (3 μg/μl) infused into the left MFB at 1.2 mm posterior, 1.2 mm lateral to bregma and −4.8 to −5.2 mm ventral from the dural surface using 33-gauge cannulas attached to a computerized syringe pump at a rate of 0.2 μl/min. The cannulas was left in place for 5 min and then slowly removed. Mice were sutured and allowed to recover on a heating pad, until they could ambulate. The great majority of mice showed a pronounced counter-clockwise rotation during this immediate after lesion recovery period. The postoperative mortality of 35% was likely attributable to the profound aphagia and adipsia (Lundblad et al., 2004). This prevented our intended littermate comparisons. However, the mice had been backcrossed four generations to C57BL/6 mice. Thus, their predicted 87.5% genetic homogeneity validated the wt to RGS9$^{-/-}$ comparisons in the absence of littermate pairings.

As illustrated in Figure 1*C*, 8 weeks after lesion, 19 wt and 10 RGS9$^{-/-}$ mice began an ascending L-dopa/benserazide dosing regimen (1–6 mg/kg). Several times during each dose, mice were assessed for L-dopa-induced AIM using a 0–4 AIM rating scale (Lundblad et al., 2004) according to the methodology developed for the rat AIMs, reaching inter-rater reliability measures of 90%. After two spaced challenges at the highest, 6 mg/kg dose, mice were killed at the height of AIM, 40 min after L-dopa injection by a lethal dose of chloral hydrate followed by transcardial perfusion of 4% paraformaldehyde.

TH immunohistochemistry. Brains were removed from the skull, and processed for TH immunohistochemistry (Waugh et al., 2005) to assess lesion quality. Image analysis of TH immunoreactivity (chromogen-based) in dorsal striatum from the lesioned and unlesioned sides of three spaced coronal sections was used to quantify the degree of lesion using a CCD camera (ExwaveHAD; Sony) and NIH Image software (version 1.61). Only mice showing a decrease of TH staining >90% were retained for final analysis.

Statistical analysis

For multiple comparisons of behavioral ratings, data were compared using a repeated measures ANOVA followed by Fisher's *post hoc* tests. Automated locomotor activity countings were analyzed using two-way ANOVA followed by Bonferroni's *post hoc* tests. The Western blot data were analyzed by one-way ANOVA. All data were normally distributed, and significance levels of *t* test comparisons were adjusted for inequality of variances when appropriate. The null hypothesis was rejected when $p < 0.05$. These analyses were completed using STATA program (Intercooled Stata 9.0; Stata, College Station, TX).

Results

The macaque model of PD and LID

We used 4 experimental groups as previously described (Bezard et al., 2003; Aubert et al., 2005) (Fig. 1): (1) Unlesioned control; (2) MPTP/vehicle; (3) MPTP/nondyskinetic and (4) MPTP/dyskinetic. The animals used for the Western blotting study have been presented in previous publications. Their motor behavior (Bezard et al., 2003), the extent of lesion (Guigoni et al., 2005a) and various postmortem indexes have been published using this brain bank (Aubert et al., 2005, 2007) (Table 1).

The MPTP/dyskinetic monkeys used for the viral manipulation behavioral study were specifically generated. Their degree of parkinsonism and dyskinesia severity were comparable with the other groups ($p > 0.5$) (Table 1). They presented choreic-athetoid (characterized by constant writhing and jerking motions), dystonic and sometimes ballistic movements (large-amplitude flinging, flailing movements). At the peak of dose (80–150 min after injection), dystonic rolling and writhing on the cage floor were common. Dyskinesia developed by MPTP-lesioned animals was similar to the LID observed in PD patients. The extent of lesion was checked for ensuring they had identical parameters to those of the animals used in the Western blot analysis (Guigoni et al., 2005a) (Table 1).

Changes in RGS9–2 in primate models of PD and LID

How RGS expression, and RGS9–2 in particular, is regulated in PD and LID is almost unknown. We first assessed the status for changes in RGS9–2 expression after DA denervation and DA denervation followed by long-term L-dopa/carbidopa treatment. Western blot analysis of total putamen samples from the four groups showed that RGS9–2 content was not significantly affected by the MPTP treatment or the chronic L-dopa/carbidopa treatment (Fig. 2*A*). We also found no evidence for denervation or L-dopa/carbidopa-induced alterations in the abundance of other RGS proteins or RGS9–2's binding partner, Gβ5 (Fig. 2*B–E*). Together, the Western blot findings indicate that both DA depletion and additional chronic L-dopa/carbdopa treatment do

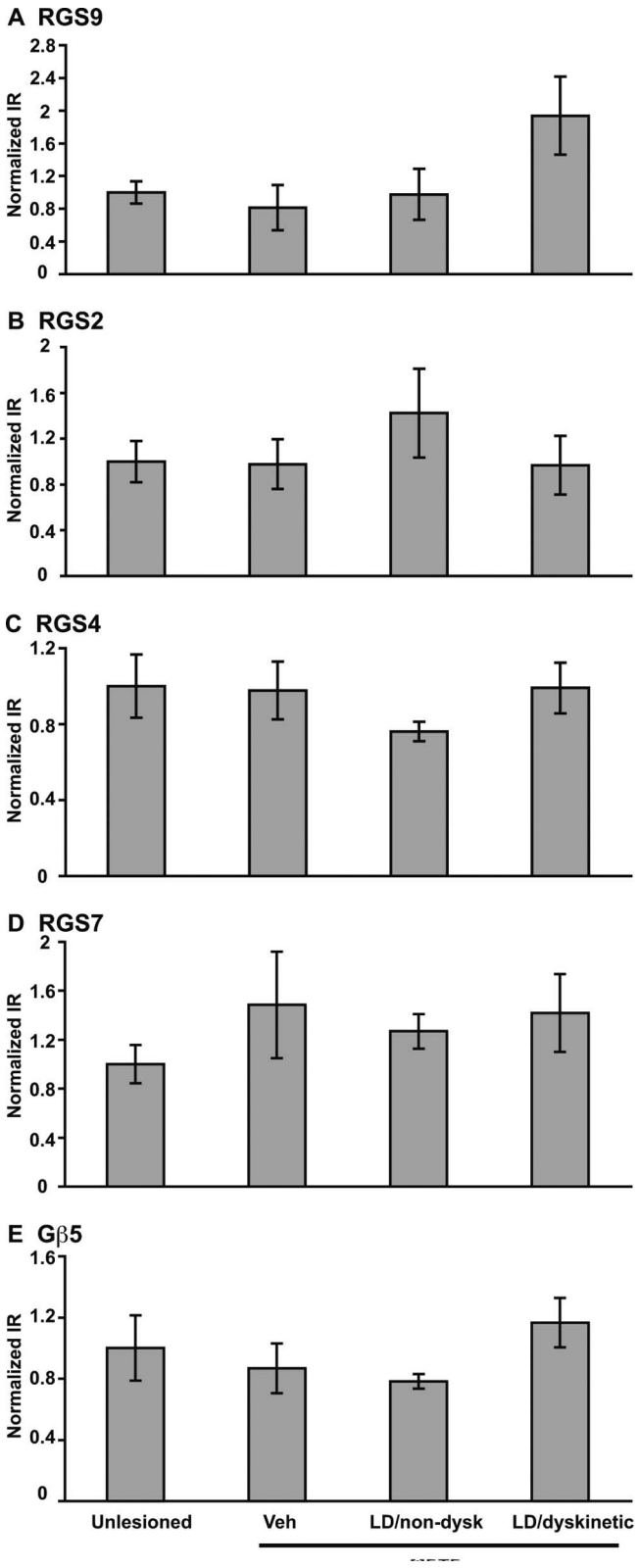

Figure 2. Striatal RGS levels in the macaque model of PD and LID. ***A–E***, Densitometric quantification of RGS9–2 (***A***), RGS2 (***B***), RGS4 (***C***), RGS7 (***D***), and Gβ5 (***E***) in striatal caudate/putamen extracts from unlesioned and lesioned/MPTP-treated monkeys chronically injected with vehicle or L-dopa/carbidopa (LD). The chronic L-dopa/carbidopa-treated group is further divided into nondyskinetic and dyskinetic groups. Monkeys were killed 1 h after last drug injection, i.e., at the peak of behavioral manifestations. RGS immunoreactivities were normalized to total Gβ immunoreactivity and are expressed as mean ± SEM. Statistical analyses were one-way ANOVA. ***A***, $F_{(3,17)} = 2.47$, $p = 0.104$; ***B***, $F_{(3,17)} = 0.65$, $p = 0.59$; ***C***, $F_{(3,17)} = 0.62$, $p = 0.61$; ***D***, $F_{(3,17)} = 0.60$, $p = 0.62$; ***E***, $F_{(3,17)} = 0.99$, $p = 0.42$.

not affect the regulation of RGS9–2, opening the way for modulating its expression.

Viral vector-mediated RGS9–2 expression diminishes LID intensity in MPTP monkeys

Our central hypothesis is that increased RGS9–2 expression will diminish the severity of dyskinesia elicited by the D1R/D2R indirect agonist L-dopa. To test this prediction, we used transient herpes simplex virus (HSV)-mediated RGS9–2 expression (Rahman et al., 2003) in motor striatum of MPTP-L-dopa/carbidopa treated-dyskinetic macaques (MPTP/dyskinetic). Before the HSV-mediated expression, parkinsonian disability scores in both the OFF (i.e., before L-dopa/carbidopa administration) and ON states (i.e., after L-dopa/carbidopa administration) and LID score in the ON state were indistinguishable between the HSV-RGS9–2 and HSV-LacZ groups (Fig. 3*A*,*B*). However, 4 d after intraputaminal injection, i.e., at the supposed height of the viral-mediated expression (Carlezon et al., 2000), monkeys expressing RGS9–2 had significantly less intense LID than monkeys expressing control LacZ (Fig. 3*D*) ($p < 0.05$). The anti-parkinsonian action of L-dopa/carbidopa did not differ between these two groups (Fig. 3*C*) at any time point. There was also a significant decrease in locomotor activity counts during ON state in the HSV-RGS9–2 animals compared with the HSV-LacZ group (Fig. 3*G*) ($p < 0.05$). One should note, however, that activity counts are still above the activity displayed before MPTP intoxication (Fig. 3*G*) as it integrates both the anti-parkinsonian response and the hyperactivity/LID displayed by the monkeys. Animals were then maintained on L-dopa/carbidopa for 2 weeks (7:00 A.M. daily), i.e., at a time when HSV-mediated RGS9–2-driven expression had ceased (Carlezon et al., 1997). After cessation of viral-mediated expression, HSV-RGS9–2 and HSV-LacZ monkeys exhibited LID intensities that were again, indistinguishable (Fig. 3*F*). These results show that viral vector-mediated RGS9–2 expression in macaque motor striatum (Fig. 3*H*) diminishes LID intensity in the macaque model without interfering with the anti-parkinsonian action of the D1R/D2R indirect agonist L-dopa.

Viral vector-mediated RGS9–2 expression diminishes D2R agonist-induced dyskinesia intensity and anti-parkinsonian effect in MPTP monkeys

RGS9–2 modulates DA signaling in the basal ganglia by terminating preferentially D2R signaling (Rahman et al., 2003; Kovoor et al., 2005). We predicted that viral-mediated expression of RGS9–2 should reduce the ability of a D2R agonist to improve the parkinsonian symptoms. To test this prediction, we performed behavioral assessments of the D2R/D3R agonist, ropinirole parallel to our assessments of L-dopa/carbidopa effects. Whereas the L-dopa/carbidopa challenges were made daily in the morning (7:00 A.M.), monkeys received a second daily challenge of the D2R/D3R agonist ropinirole (Rascol et al., 2000) in the afternoon (3:00 P.M.), i.e., when animals had returned to their morning OFF score [note that all OFF PD scores are identical throughout the whole experiment whatever the day or morning/afternoon assessment (Figs. 3*A–C*, 4*A–C*)]. As described above, before the HSV transfection, parkinsonian disability scores in both the OFF and ON (i.e., after ropinirole administration) states and dyskinesia score in the ON state were indistinguishable between the HSV-RGS9–2 and HSV-LacZ groups (Fig. 4*A*,*B*). However, 4 d after intracranial injection of virus, HSV-RGS9–2 monkeys were significantly less improved by the ropinirole administration than HSV-LacZ mon-

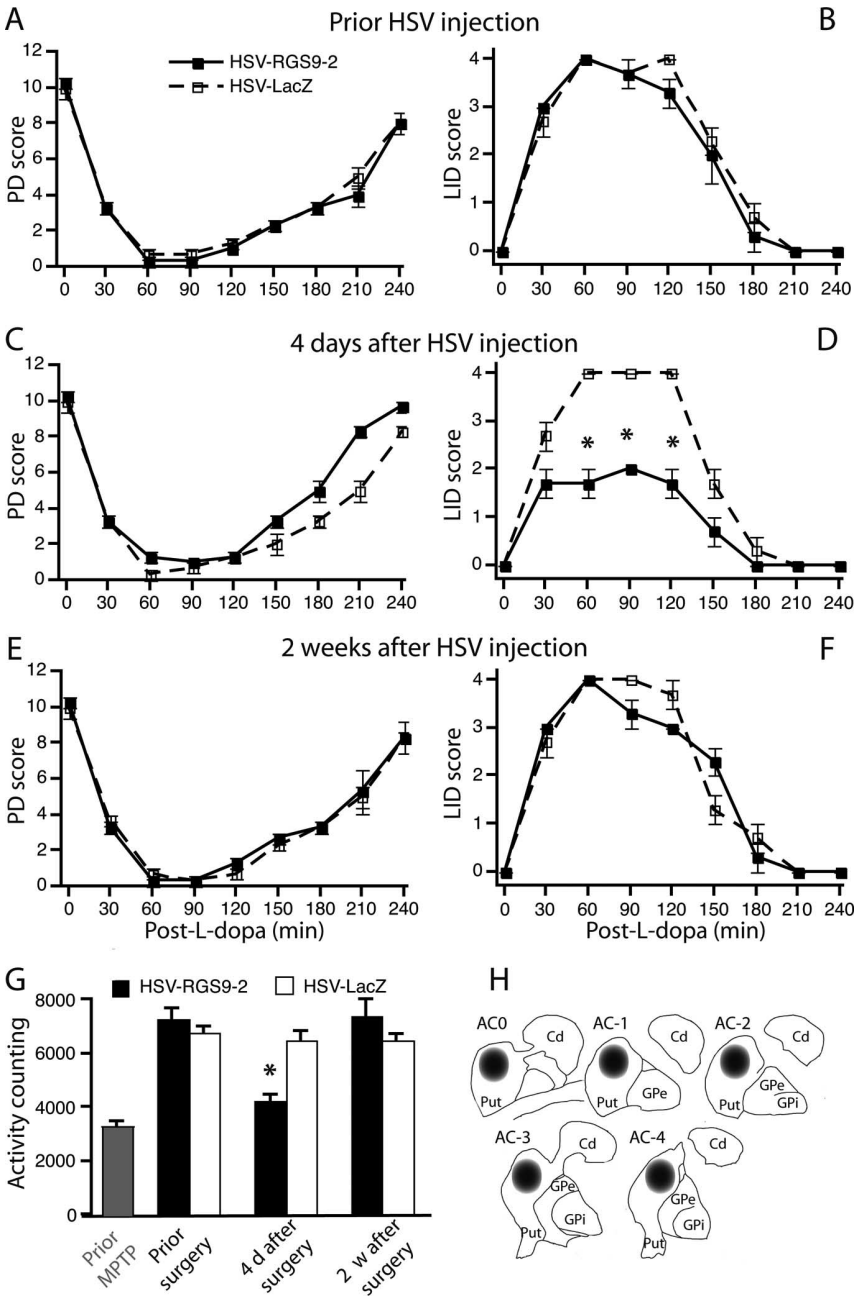

Figure 3. Viral-mediated RGS9–2 expression in macaque motor striatum decreases LID intensity. Behavioral data expressed as mean ± SEM are analyzed by repeated-measures ANOVA followed by Fisher's *post hoc* tests. ***A***, ***B***, Before HSV injections, dyskinetic MPTP-treated macaques show indistinguishable decreases in parkinsonian disability score (***A***; virus type, $F_{(1,53)} = 0.93$, $p = 0.34$; time, $F_{(8,53)} = 134.93$, $p < 0.0001$; interaction, $F_{(8,53)} = 0.43$, $p = 0.89$) and increases in dyskinesia score after an L-dopa challenge (***B***; virus type, $F_{(1,53)} = 0.90$, $p = 0.34$; time, $F_{(8,53)} = 98.72$, $p < 0.0001$; interaction, $F_{(8,53)} = 0.67$, $p = 0.71$). $n = 3$ macaques per group. ***C***, ***D***, During the height of HSV-mediated overexpression in dorsolateral striatum, 4 d after infection, RGS9–2 overexpressing macaques show comparable anti-parkinsonian response to L-dopa (***C***; virus type, $F_{(1,53)} = 31.36$, $p < 0.0001$; time, $F_{(8,53)} = 159.66$, $p < 0.0001$; interaction, $F_{(8,53)} = 3.64$, $p < 0.0001$) and diminished LID scores (***D***; virus type; $F_{(1,53)} = 104.14$, $p < 0.0001$; time, $F_{(8,53)} = 85.0$, $p < 0.0001$; interaction, $F_{(8,53)} = 11.57$, $p < 0.0001$) relative to LacZ overexpressing controls (*$p < 0.05$). ***E***, ***F***, At 2 weeks after infection, when overexpression has ceased, formerly RGS9–2 and LacZ groups are again indistinguishable (PD scores: virus type, $F_{(1,53)} = 0.23$, $p = 0.63$; time, $F_{(8,53)} = 96.85$, $p < 0.0001$; interaction, $F_{(8,53)} = 0.22$, $p = 0.98$; LID scores: virus type, $F_{(1,53)} = 0.14$, $p = 0.70$; time, $F_{(8,53)} = 133.96$, $p < 0.0001$; interaction, $F_{(8,53)} = 3.04$, $p < 0.05$). ***G***, Automated locomotor activity counts recorded in parallel to the video recordings show that, 4 d after surgery, RGS9–2 overexpressing macaques display less hyperactivity (*$p < 0.05$). The gray column represents activity counts in the normal state, i.e., previous MPTP intoxication. Data expressed as mean ± SEM are analyzed by two-way ANOVA, followed by Bonferroni's *post hoc* tests. Virus type, $F_{(1,17)} = 0.98$, $p = 0.34$; time, $F_{(2,17)} = 13.65$, $p < 0.0.001$; interaction, $F_{(2,17)} = 11.40$, $p < 0.01$. ***H***, Schematic representation of targeted area of motor striatum during stereotaxic surgery. Five different rostrocaudal levels from anterior commissural (AC) to 4 mm caudal to AC (AC-4 mm) received 10 μl of either HSV-RGS9–2 or HSV-LacZ 3 mm above the virtual horizontal line passing through AC and posterior commissural. Put, Putamen; Cd, caudate nucleus; GPe, globus pallidus externalis; GPi, globus pallidus internalis.

keys (Fig. 4*C*). Furthermore they showed dramatically reduced locomotor activity (Fig. 4*G*) that fell far below the activity displayed in the normal unlesioned situation (Fig. 4*G*). At the same time, HSV-RGS9–2 monkeys were significantly less dyskinetic than HSV-LacZ monkeys (Fig. 4*D*) ($p < 0.05$). Animals were then maintained on ropinirole for 2 weeks (3:00 P.M. daily), i.e., at a time when HSV-mediated RGS9–2 expression had ceased (Carlezon et al., 1997). After cessation of viral-mediated expression, HSV-RGS9–2 and HSV-LacZ monkeys exhibited dyskinesia intensities that were again, indistinguishable (Fig. 4*E*). These results show that HSV-mediated RGS9–2 expression decreases dyskinesia but at the expense of the D2R agonist-mediated anti-parkinsonian effects.

Time course of HSV-mediated gene expression in 6-OHDA-lesioned rats

The above experiments were conducted on the basis of a timed viral-mediated expression of RGS9–2 (Carlezon et al., 1997; Barrot et al., 2002). A time course study of HSV-mediated expression in monkey was ethically not possible. We thus assessed it in unilateral 6-OHDA-lesioned rats with AIMs (Rahman et al., 2003) caused by chronic L-dopa/benserazide treatment (see timeline in Fig. 1*B*). Before the HSV injection, AIM intensities were indistinguishable among animals destined to be injected with HSV-RGS9–2 or HSV-LacZ groups (Fig. 5*A*,*B*). However, 4 d after intracranial injection of virus, i.e., at the height of transgene expression (Carlezon et al., 1997) as illustrated in Figure 5*D*, HSV-RGS9–2 rats had significantly less intense L-dopa/benserazide-induced AIMs than control HSV-LacZ rats (Fig. 5*C*). Two weeks after HSV injection, HSV-mediated expression had ceased (Carlezon et al., 1997) (Fig. 5*F*) and AIM intensities were again indistinguishable between the HSV-RGS9–2 and HSV-LacZ groups (Fig. 5*E*). Those animals exhibited comparable extent of lesion (Fig. 5*G*). These results indicate that the temporal expression of HSV-mediated transgene is consistent with that of the AIM severity in HSV-RGS9–2 6-OHDA-lesioned rats which, in turn, is consistent with that of the LID severity in HSV-RGS9–2 MPTP monkeys (Fig. 3*B*,*D*,*F*). Thus these observations support the suitability of the chosen time points in the monkey study.

The cellular expression as well as the level of HSV-mediated RGS9–2 expression remain an issue. Published data demonstrate that neuronal infection of HSV-RGS9–2 induces RGS9–2 protein that comigrates with endogenous RGS9–2 by SDS-PAGE and that the overexpressed RGS9–2 is biologically active

(Rahman et al., 2003; Zachariou et al., 2003). Furthermore, although technical limitations precluded visualizing HSV-mediated RGS9–2 overexpression in striatal MSNs, a variant of the RGS9–2 virus containing an N terminus Myc-tag permitted immunohistochemical visualization of MSNs densely expressing Myc-RGS9–2 (Fig. 5*H*) (supplemental Fig. 2, available at www.jneurosci.org as supplemental material). Thus, wild-type HSV-RGS9–2 is likely to also target MSNs.

RGS9–2 deletion increases L-dopa-induced AIMs in 6-OHDA-lesioned mice

The monkey experiment shows that HSV-mediated RGS9–2 expression decreases LID. The reverse hypothesis predicts that reduced RGS9–2 activity will increase the expression of LID as suggested by Kovoor et al. (2005). To test this prediction, we combined mouse genetics, unilateral 6-OHDA lesions and behavioral analyses (schematically depicted in Fig. 1*C*). Four weeks after 6-OHDA injection (Lundblad et al., 2004), cylinder test analysis showed a clear bias of ipsilateral forelimb use that was indistinguishable between wt and RGS9$^{-/-}$ 6-OHDA-lesioned mice (data not shown). Open-field analysis showed rotational bias away from the lesioned side that was again indistinguishable between wt and RGS9$^{-/-}$ mice (data not shown). At 8 weeks after lesion, mice began an ascending, once daily L-dopa/benserazide dosing regimen (1, 1.5, 2, 3 and 6 mg/kg L-dopa) (for timeline, see Fig. 1*C*) and were rated for both rotational behavior and axial/forelimb AIM severity (Lundblad et al., 2004). As can be seen in Figure 6, *A* and *B*, rotational behavior, an index of the anti-parkinsonian response to L-dopa/benserazide, was comparable between wt and RGS9$^{-/-}$ mice, suggesting again that anti-parkinsonian response to L-dopa/benserazide is not affected by changes in RGS9–2 levels. However, when assessing axial and forelimb AIM, the difference reached statistical significance, with the RGS9$^{-/-}$ mice exhibiting greater AIM than their wt littermates (Fig. 6*C*,*D*). *Post hoc* analysis of the dose-averaged AIM (Fig. 6*D*) showed that axial/forelimb AIM were significantly different at the 1 mg/kg dose.

Discussion

Our findings suggest that increasing RGS9–2 activity, a GTPase accelerating protein (GAP) for Gα subunits, can markedly attenuate LID in response to L-dopa, without compromising L-dopa's therapeutically beneficial anti-parkinsonian effects. In addition, our findings demonstrate that

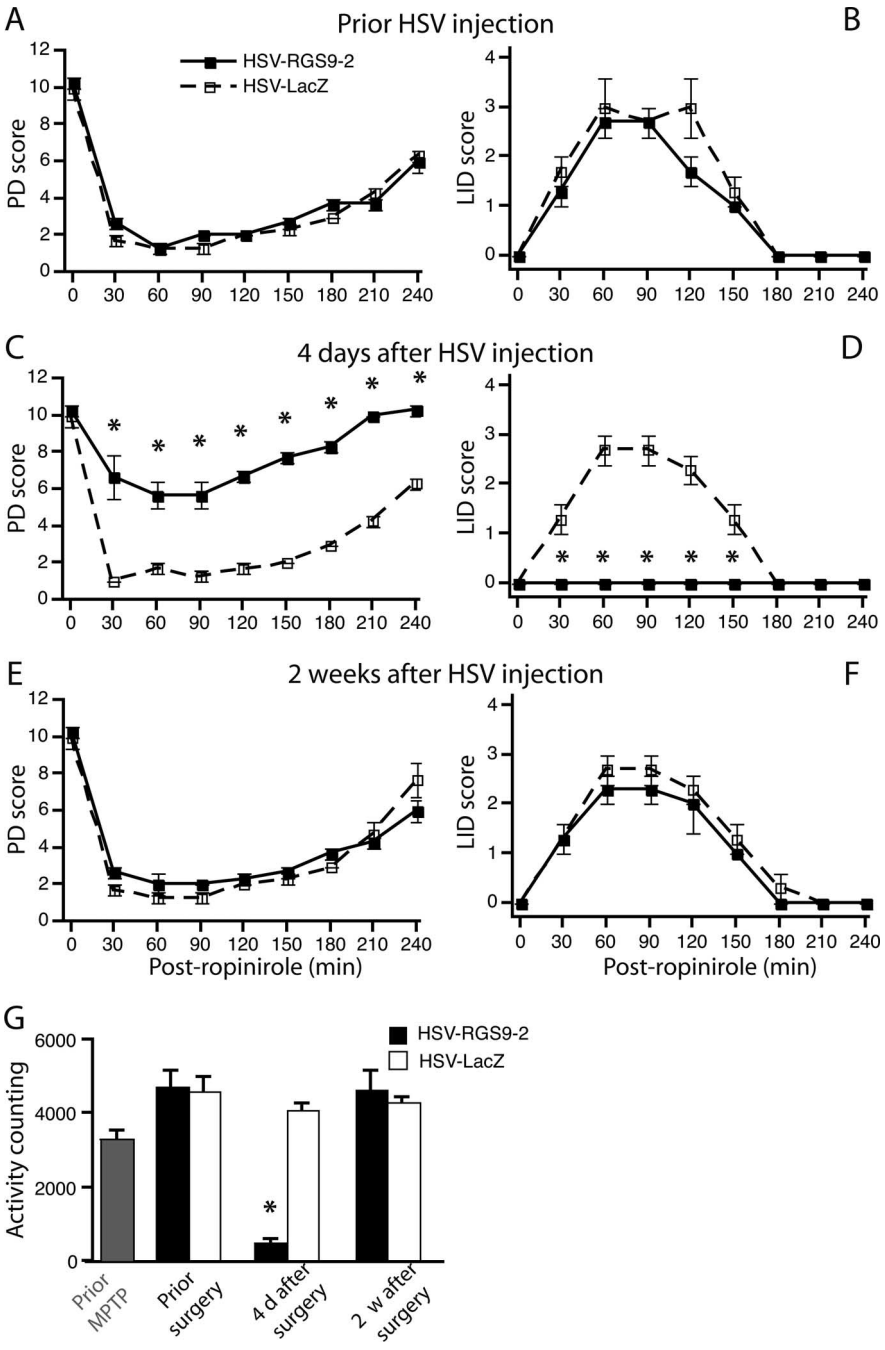

Figure 4. Viral-mediated RGS9–2 expression in macaque motor striatum decreases the intensity of ropinirole-induced dyskinesia at the expense of anti-parkinsonian effect. Behavioral data expressed as mean ± SEM are analyzed by repeated-measures ANOVA, followed by Fisher's *post hoc* tests. ***A***, ***B***, Before HSV injections, dyskinetic MPTP-treated macaques show indistinguishable decrease in parkinsonian disability score (***A***; virus type, $F_{(1,53)} = 2.0$, $p = 0.17$; time, $F_{(8,53)} = 145.22$, $p < 0.0001$; interaction, $F_{(8,53)} = 1.25$, $p = 0.30$) and increase in dyskinesia score after a ropinirole challenge (***B***; virus type, $F_{(1,53)} = 3.77$, $p = 0.06$; time, $F_{(8,53)} = 37.21$, $p < 0.0001$; interaction, $F_{(8,53)} = 1.17$, $p = 0.34$). $n = 3$ macaques per group. ***C***, ***D***, During the height of HSV-mediated overexpression in dorsolateral striatum, 4 d after infection, RGS9–2 overexpressing macaques show dramatically diminished anti-parkinsonian responses to ropinirole (***C***; virus type, $F_{(1,53)} = 423.53$, $p < 0.0001$; time, $F_{(8,53)} = 53.13$, $p < 0.0001$; interaction, $F_{(8,53)} = 6.82$, $p < 0.0001$) and diminished LID scores (***D***; virus type, $F_{(1,53)} = 192.20$, $p < 0.0001$; time, $F_{(8,53)} = 23.0$, $p < 0.0001$; interaction, $F_{(8,53)} = 23.0$, $p < 0.0001$) relative to LacZ overexpressing controls (*$p < 0.05$). ***E***, ***F***, At 2 weeks after infection, when overexpression has ceased, formerly RGS9–2 and LacZ groups are again indistinguishable (PS scores: virus type, $F_{(1,53)} = 1.20$, $p = 0.28$; time, $F_{(8,53)} = 89.77$, $p < 0.0001$; interaction, $F_{(8,53)} = 1.72$, $p = 0.13$; LID scores: virus type, $F_{(1,53)} = 2.08$, $p = 0.16$; time, $F_{(8,53)} = 32.46$, $p < 0.0001$; interaction, $F_{(8,53)} = 0.21$, $p = 0.98$). ***G***, Automated locomotor activity counts recorded in parallel to the video recording shows that, 4 d after surgery, RGS9–2 overexpressing macaques do not move after ropinirole challenge (*$p < 0.05$). The gray column represents activity counts in the normal state, i.e., previous MPTP intoxication. Data expressed as mean ± SEM are analyzed by two-way ANOVA, followed by Bonferroni's *post hoc* tests. Virus type, $F_{(1,17)} = 16.0$, $p < 0.01$; time, $F_{(2,17)} = 33.69$, $p < 0.0.0001$; interaction, $F_{(2,17)} = 24.14$, $p < 0.0001$

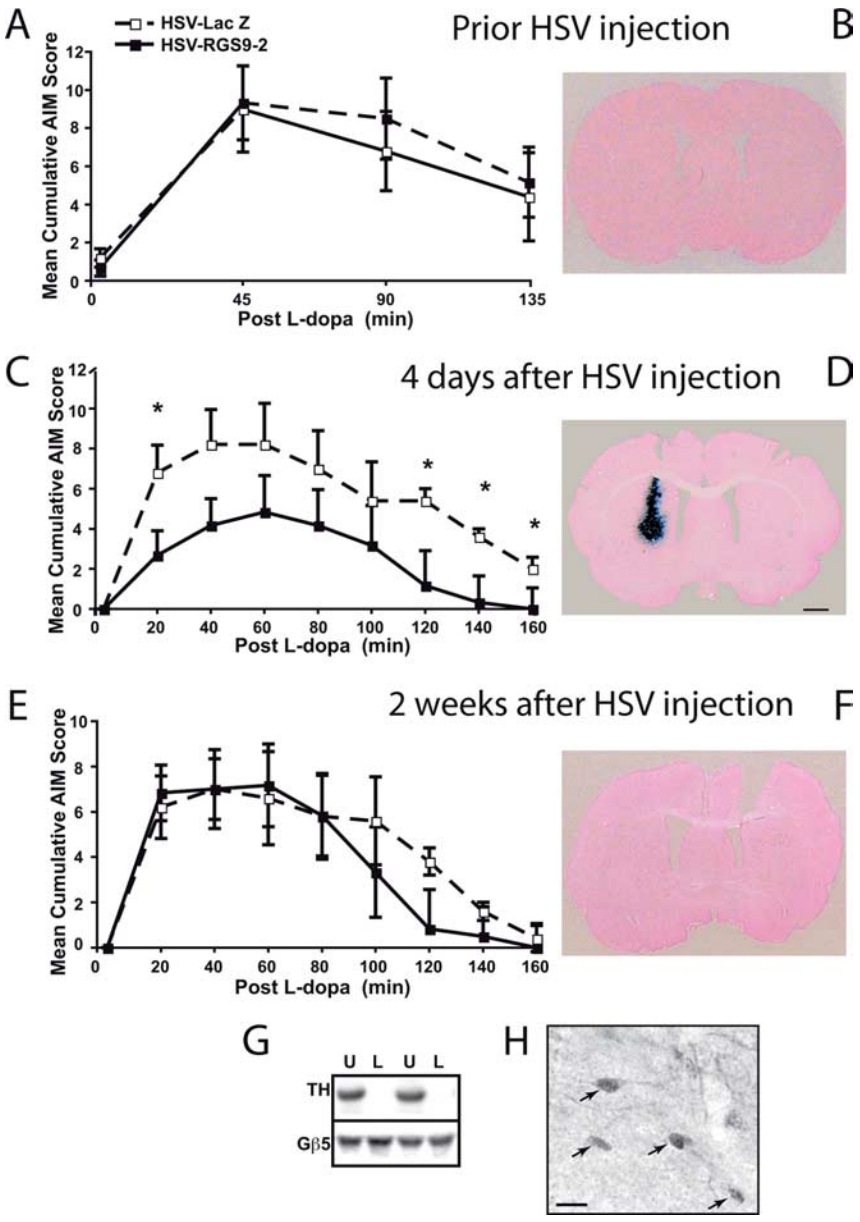

Figure 5. Viral-mediated RGS9–2 overexpression in rat striatum decreases AIM intensities. ***A***, Rats made dyskinetic by 6-OHDA lesion followed by 4 weeks of daily L-dopa/benserazide administration (8 mg/kg) show indistinguishable AIM intensities in response to L-dopa before HSV injections. Shown are the average cumulative AIM scores (rotational + axial + forelimb + orolingual − total possible 16). ***B***, Nuclear fast red-counterstained β-galactosidase staining before HSV-LacZ injection. ***C***, During the height of HSV-mediated overexpression in dorsolateral striatum, 4 d after HSV infection, RGS9–2 overexpressing rats show diminished cumulative AIM scores relative to LacZ overexpressing controls. ***D***, Nuclear fast red-counterstained β-galactosidase staining 4 d after HSV-LacZ injection showing intense staining in the dorsal striatum. Scale bar, 1 mm. ***E***, At 2 weeks after HSV infection, when overexpression has ceased, formerly RGS9–2 and LacZ groups have AIM scores that are again indistinguishable. ***F***, Nuclear fast red-counterstained β-galactosidase staining 2 weeks after HSV-LacZ injection showing no staining as expression has ceased. ***G***, Typical results of TH immunoblotting on the lesioned (L) and unlesioned (U) sides of experimental rats. Gβ5 serves as a loading control. ***H***, Immunohistochemical localization of infected rat dorsal striatal cells (arrows) overexpressing N-terminal Myc-tagged RGS9–2 suggest that infected cells are principally of the MSN class. Scale bar, 13 μm. Data expressed as mean ± SEM are analyzed by repeated-measures ANOVA, followed by Fisher's *post hoc* tests; $^*p < 0.05$. $n = 6$ and 5 for HSV-RGS9–2 and HSV-LacZ groups, respectively. ***A***, Virus type, $F_{(1,43)} = 0.08$, $p = 0.78$; time, $F_{(3,43)} = 15.64$, $p < 0.0.0001$; interaction, $F_{(5,43)} = 0.26$, $p = 0.85$. ***C***, $F_{(1,98)} = 10.54$, $p = 0.03$; time, $F_{(8,98)} = 10.76$, $p < 0.0001$; interaction, $F_{(10,98)} = 3.04$, $p < 0.01$. ***E***, $F_{(1,98)} = 0.23$, $p = 0.64$; time, $F_{(8,98)} = 24.12$, $p < 0.0001$; interaction, $F_{(10,98)} = 1.11$, $p = 0.36$.

the benefit of increased RGS9–2 activity is restricted to the combined D1/D2-like agonist L-dopa. Enhanced RGS9–2 activity actually diminishes the anti-parkinsonian properties of the D2/D3 agonist ropinirole.

Consistent behavioral effects across three animal models

A key add-on of our study is the use of three validated animal models of PD and LID. The significant, albeit small, difference in AIM severity between wt and RGS9$^{-/-}$ mice is very similar to that reported previously (Kovoor et al., 2005) and supports the concept that RGS9–2 deletion increases L-dopa-induced AIMs. Overexpressing RGS9–2 in the monkey model of LID clearly diminished LID intensity as was the case for AIMs in the L-dopa-treated 6-OHDA-lesioned rat. However, are those effects specific to LID behaviors? The monkey experiments were specifically designed to address this critical question because measures of both locomotor performance and maintenance of the anti-parkinsonian action of L-dopa were performed concomitantly with measures of LID. In the monkey experiments, 3 different panels are presented for each time point (before surgery, at peak of expression, and when expression has returned to baseline): (1) the assessment of the parkinsonian abnormalities in response to L-dopa (Fig. 3*A*,*C*,*E*) and ropinirole (Fig. 4*A*,*C*,*E*), (2) the assessment of the dyskinesia severity in response to L-dopa (Fig. 3*B*,*D*,*F*) and ropinirole (Fig. 4*B*,*D*,*F*) and (3) the automated recording of locomotor activity in response to L-dopa (Fig. 3*G*) and ropinirole (Fig. 4*G*). Although both PD and LID scores are fine grained tools for addressing the quantitative and qualitative severity of the symptoms (Bezard et al., 2003), the automated recording of locomotor activity integrates both "normal" and "hyperactive" components (for a clear example, see Bezard et al., 2003). Therefore the decreased activity after L-dopa treatment with RGS9–2 expression corresponds to the suppression of the hyperkinetic component recorded before HSV transfection.

In the same way, we show that, although the anti-parkinsonian activity of the L-dopa is preserved in the overexpressing RGS9–2 animals (Fig. 3*C*), this beneficial activity is diminished when the D2/D3 dopamine agonist ropinirole is administered (Fig. 4*C*). Thus, the lack of dyskinesia is likely the consequence of the loss of antiparkinsonian activity. In other words, the lowered anti-parkinsonian effect of ropinirole with RGS9–2 overexpression proves that, if translated to the clinic, the strategy should be used together with either L-dopa, the mixed D1/D2 agonist apomorphine (recently marketed in the US) or a direct D1 agonist (not yet available) but NOT with a D2/D3 DA agonist (ropinirole, pramipexole, carbergoline, rotigotine, etc.). This disparity in efficacy between D2/D3 and mixed (L-dopa) agonists is strong support for our hypothesis that RGS9–2 amelioration of LID occurs via its actions at D2/D3 expressing neurons.

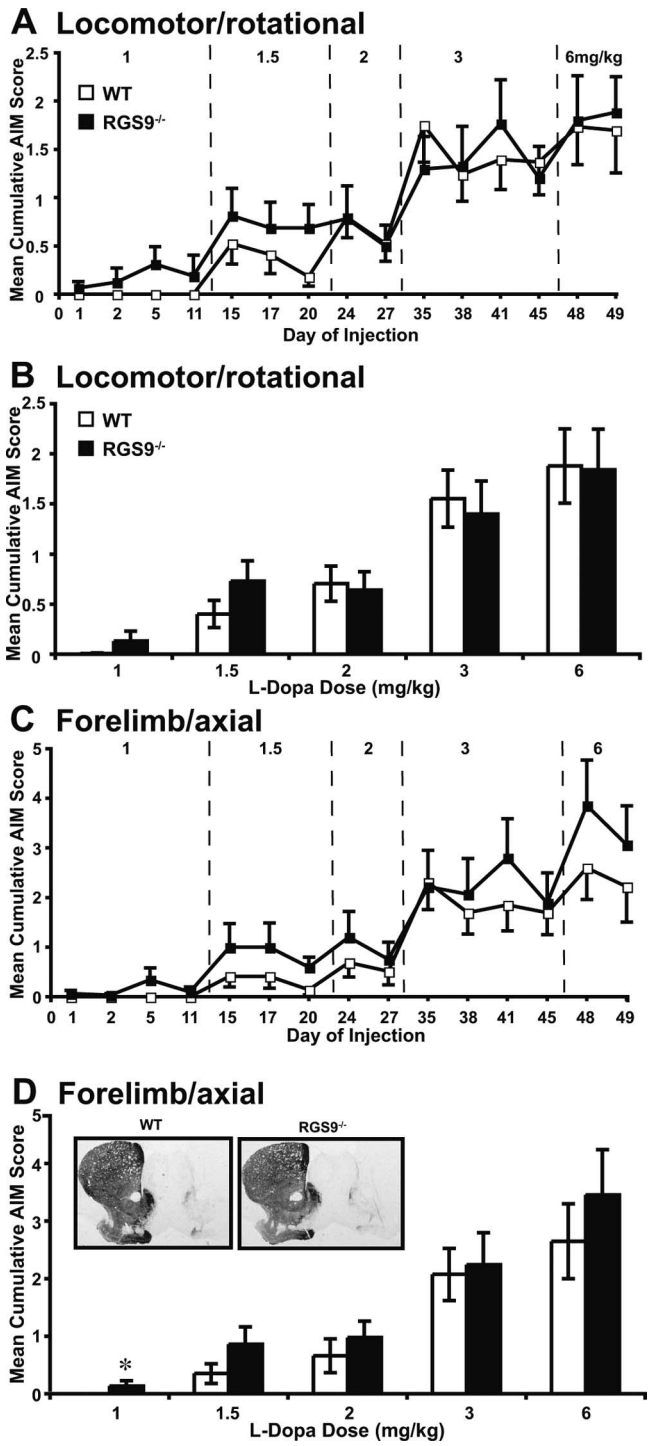

Figure 6. RGS9 $^{-/-}$ mice are more sensitive to the AIM-inducing properties of L-dopa than their wt littermates. Unilateral 6-OHDA lesioned mice were treated once daily with L-dopa on an ascending dose regimen (1, 1.5, 2, 3, and 6 mg/kg). ***A–D***, Mice were assayed intermittently two to four times per dose for rotational behavior (***A***, ***B***) and the presence of forelimb/axial AIM (***C***, ***D***). Days after initiation of daily L-dopa treatments are indicated on the *x*-axis (***A***, ***C***), with the different doses across time separated by vertical dashed lines and specific doses indicated at the top of the graphs (***A***, ***C***). Rotational behavior (***B***) and L-dopa-induced AIM scores per dose per genotype (***D***) were averaged across at least two observations for each dose. Inset in ***D*** shows typical TH immunoreactivity on lesioned side (right) and unlesioned side (left). Data are expressed as mean ± SEM and are analyzed by repeated-measures ANOVA. ***B***, Genotype, $F_{(1,95)} = 2.32$, $p = 0.13$; dose, $F_{(4,95)} = 37.98$, $p < 0.001$; interaction, $F_{(6,95)} = 0.65$, $p = 0.63$. ***D***, Genotype, $F_{(1,95)} = 3.95$; $p < 0.05$; Fisher's *post hoc* test, $^*p < 0.05$; dose, $F_{(4,95)} = 35.94$, $p < 0.0001$; interaction, $F_{(6,95)} = 0.36$, $p = 0.83$. $n = 11$, 8 for wt and RGS9 $^{-/-}$, respectively.

Neuroanatomical and functional implications

Our findings can be explained by the sole RGS9–2-mediated attenuation of D2R signaling in MSNs (Fig. 5*H*). Importantly, endogenous RGS9–2 protein is expressed in both D1 (substance P) and D2R (enkephalin) containing MSNs (Rahman et al., 2003). The question remains as to the identity of the MSNs and of the other cell types that can be transfected by the HSV virus. We showed previously in the primate (1) that striatofugal pathways are not as segregated (Nadjar et al., 2006) as previously thought (Gerfen et al., 1990) and (2) that a significant proportion of MSNs should coexpress D1R and D2R (Aizman et al., 2000; Nadjar et al., 2006). This raises the possibility that, even if HSV-mediated RGS9–2 expression was truly preferentially modulating D2R, HSV-mediated RGS9–2 expression (1) affects both striatofugal pathways anyway and (2) modulates the activity of the MSNs coexpressing D1R and D2R. RGS9–2, however, inhibits other GPCRs, such as μ-opioid receptor (Zachariou et al., 2003; Psifogeorgou et al., 2007) that colocalize with D1R in the striatum (Lindskog et al., 1999). As a common integrator of those signals is DARPP-32 (Lindskog et al., 1999), how enhanced RGS9–2 expression in D1R enriched neurons would effect basal ganglia function is likely attributable to complex regulation of its phosphorylation. Future studies should more fully elucidate the mechanism of RGS9–2's regulation of basal ganglia information flow.

Other neuronal types can be transfected in the striatum, such as the DA striatal interneurons whose fate have yet to be determined (Huot et al., 2007), and the two major interneuron populations: the parvalbumin-positive GABAergic fast spiking interneurons and the cholinergic interneurons, both of which shape MSN activity (Centonze et al., 2003; Mallet et al., 2005). Although GABAergic fast spiking interneurons mainly express D1R (Centonze et al., 2003), the cholinergic interneurons are interesting candidates. As striatal DA levels fall, the D2R-mediated inhibitory tone decreases (MacKenzie et al., 1989) and striatal acetylcholine levels rise. These inter-related responses exacerbate motor symptoms (Barbeau, 1962). L-dopa or ropinirole supplementation should restore this inhibitory tone, but one could hypothesize that increasing RGS9–2 levels in these neurons in dyskinetic monkeys would terminate D2R signaling too rapidly and actually reproduce the pathological situation, exacerbating PD symptoms as we found for ropinirole in our monkey study (Fig. 4).

Although the effects of HSV-mediated expression of transgenes have primarily been attributed to postsynaptic expression, others have described HSV-mediated infection of neurons via terminal uptake (for review, see Berges et al., 2007). Given the vast volume of striatum targeted in our monkeys and the great quantity of infectious particles injected, it is conceivable that nerve endings, including the remaining DA terminals (Guigoni et al., 2005a), were infected. The role (1) for RGS9–2 in regulating those presynaptic D2 autoreceptors or (2) for RGS9–2 in modulating GPCRs in nondopaminergic striatal nerve endings is an issue that has yet to be resolved. Nevertheless, the current understanding of HSV infection favors postsynaptic mediation of RGS9–2's anti-LID properties as presynaptic HSV transgene expression only occurs after long postinfection latencies (Berges et al., 2007), latencies that are not compatible with the short duration of the present experiments (2 weeks) (Fig. 1).

Functional specificity of RGS proteins in striatum.

Although our findings suggest that enhanced RGS9–2 activity blocks LID by inhibiting D2R signaling, RGS modulation of other GPCR signaling in basal ganglia may provide distinct paths for

treating PD and related symptoms. Indeed it is worth noting that at least 8 distinct RGS genes are expressed at moderate to high levels in striatum including RGS2, RGS4, RGS6, RGS7, RGS9–2, RGS10, RGS14 and RGSZ1 (Gold et al., 1997; Glick et al., 1998; Grafstein-Dunn et al., 2001). This list represents a functionally diverse set of RGS proteins: They modulate distinct classes of G α subunits and presumably specific GPCRs. Others have reported regulation of a subset of these RGS proteins in animal models of PD (Geurts et al., 2003; Taymans et al., 2004) as well as in human postmortem tissues (Tekumalla et al., 2001) although we failed to show such a difference in our monkey tissues. The overall lack of changes in RGS levels in monkey striatum might be attributable to the neuron-specific expression of RGS proteins as recently exemplified by Ding et al. (2006) who resolved highly localized increases in RGS4 mRNA in striatal cholinergic interneurons of DA depleted mouse. Moreover, their data support the notion that the increased RGS4 activity mediates the loss of autoreceptor tone in cholinergic interneurons after DA denervation (Ding et al., 2006). Although their data raise the possibility that drug-based blockade of RGS4 could ameliorate parkinsonian symptoms, the broad expression pattern of RGS4 (Gold et al., 1997) predicts that global perturbation of RGS4 activity will lead to numerous non-PD related side-effects.

Nevertheless, for further understanding LID pathology, it will be of great interest to determine whether and how both RGS4 and RGS9–2 activity changes in striatal cholinergic interneurons after chronic L-dopa treatment that leads to LID. The critical task of parsing the specific RGS gene functions in normal and pathological striatum will undoubtedly be very challenging. For example, we have been unable to resolve RGS9–2-specific GAP activity in mouse striatal membranes. This was true even using membranes from RGS9$^{-/-}$ mice as a negative control. This suggests that there are many GTPase accelerating proteins contributing to the total GAP activity. These other striatal GAPs should offer other potential therapeutic targets for treatment of PD and/or LID.

Conclusion

Combining these data with the highly localized striatal expression of RGS9–2, brings forth the possibility that exogenous enhancement of RGS9–2 activity could have substantial therapeutic benefits, with only minor side-effects if used with a nonselective DA agonist (L-dopa, apomorphine). Although additional experiments are needed for furthering our understanding of the biological consequences of perturbing RGS9–2 activity, significant effort needs to be devoted to understanding how RGS9–2 activity is regulated. As suggested by the findings presented here, drug-based enhancement of RGS9–2 activity could provide a novel therapeutic mechanism for increasing the utility of L-dopa therapy.

References

Abercrombie M (1946) Estimation of nuclear population from microtome sections. Anat Rec 94:239–247.

Aizman O, Brismar H, Uhlen P, Zettergren E, Levey AI, Forssberg H, Greengard P, Aperia A (2000) Anatomical and physiological evidence for D1 and D2 dopamine receptor colocalization in neostriatal neurons. Nat Neurosci 3:226–230.

Alexander GE, Crutcher MD (1990) Functional architecture of basal ganglia circuits: neural substrates of parallel processing. Trends Neurosci 13:266–271.

Aubert I, Guigoni C, Hakansson K, Li Q, Dovero S, Barthe N, Bioulac BH, Gross CE, Fisone G, Bloch B, Bezard E (2005) Increased D1 dopamine receptor signaling in levodopa-induced dyskinesia. Ann Neurol 57:17–26.

Aubert I, Guigoni C, Li Q, Dovero S, Bioulac BH, Gross CE, Crossman AR, Bloch B, Bezard E (2007) Enhanced preproenkephalin-B-derived opioid transmission in striatum and subthalamic nucleus converges upon globus pallidus internalis in L-3,4-dihydroxyphenylalanine-induced dyskinesia. Biol Psychiatry 61:836–844.

Barbeau A (1962) The pathogenesis of Parkinson's disease: a new hypothesis. Can Med Assoc J 87:802–807.

Barrot M, Olivier JDA, Perroti LI, Di Leone RJ, Berton O, Eisch AJ, Impey S, Storm D, Neve RL, Zachariou V, Nestler EJ (2002) CREB activity in the nucleus accumbens shell controls the gating of behavioral responses to emotional stimuli. Proc Natl Acad Sci USA 99:11435–11440.

Barrot M, Wallace DL, Bolanos CA, Graham DL, Perrotti LI, Neve RL, Chambliss H, Yin JC, Nestler EJ (2005) Regulation of anxiety and initiation of sexual behavior by CREB in the nucleus accumbens. Proc Natl Acad Sci USA 102:8357–8362.

Berges BK, Wolfe JH, Fraser NW (2007) Transduction of brain by herpes simplex virus vectors. Mol Ther 15:20–29.

Berman DM, Gilman AG (1998) Mammalian RGS proteins: barbarians at the gate. J Biol Chem 273:1269–1272.

Bezard E, Boraud T, Bioulac B, Gross CE (1999) Involvement of the subthalamic nucleus in glutamatergic compensatory mechanisms. Eur J Neurosci 11:2167–2170.

Bezard E, Dovero S, Prunier C, Ravenscroft P, Chalon S, Guilloteau D, Crossman AR, Bioulac B, Brotchie JM, Gross CE (2001) Relationship between the appearance of symptoms and the level of nigrostriatal degeneration in a progressive 1-methyl-4-phenyl-1,2,3,6-tetrahydropyridine-lesioned macaque model of Parkinson's disease. J Neurosci 21:6853–6861.

Bezard E, Ferry S, Mach U, Stark H, Leriche L, Boraud T, Gross C, Sokoloff P (2003) Attenuation of levodopa-induced dyskinesia by normalizing dopamine D3 receptor function. Nat Med 9:762–767.

Boraud T, Bezard E, Bioulac B, Gross CE (2001) Dopamine agonist-induced dyskinesias are correlated to both firing pattern and frequency alterations of pallidal neurones in the MPTP-treated monkey. Brain 124:546–557.

Carlezon Jr WA, Boundy VA, Haile CN, Lane SB, Kalb RG, Neve RL, Nestler EJ (1997) Sensitization to morphine induced by viral-mediated gene transfer. Science 277:812–814.

Carlezon Jr WA, Nestler EJ, Neve RL (2000) Herpes simplex virus-mediated gene transfer as a tool for neuropsychiatric research. Crit Rev Neurobiol 14:47–67.

Cenci MA (2007) Dopamine dysregulation of movement control in L-DOPA-induced dyskinesia. Trends Neurosci 30:236–243.

Cenci MA, Lee CS, Bjorklund A (1998) L-DOPA-induced dyskinesia in the rat is associated with striatal overexpression of prodynorphin- and glutamic acid decarboxylase mRNA. Eur J Neurosci 10:2694–2706.

Cenci MA, Whishaw IQ, Schallert T (2002) Animal models of neurological deficits: how relevant is the rat? Nat Rev Neurosci 3:574–579.

Centonze D, Grande C, Usiello A, Gubellini P, Erbs E, Martin AB, Pisani A, Tognazzi N, Bernardi G, Moratalla R, Borrelli E, Calabresi P (2003) Receptor subtypes involved in the presynaptic and postsynaptic actions of dopamine on striatal interneurons. J Neurosci 23:6245–6254.

Chen CK, Burns ME, He W, Wensel TG, Baylor DA, Simon MI (2000) Slowed recovery of rod photoresponse in mice lacking the GTPase accelerating protein RGS9–1. Nature 403:557–560.

Ding J, Guzman JN, Tkatch T, Chen S, Goldberg JA, Ebert PJ, Levitt P, Wilson CJ, Hamm HE, Surmeier DJ (2006) RGS4-dependent attenuation of M4 autoreceptor function in striatal cholinergic interneurons following dopamine depletion. Nat Neurosci 9:832–842.

Feger J, Ohye C, Gallouin F, Albe-Fessard D (1975) Stereotaxic technique for stimulation and recording in nonanesthetized monkeys: application to the determination of connections between caudate nucleus and substantia nigra. Adv Neurol 10:35–45.

Francois C, Yelnik J, Percheron G (1996) A stereotaxic atlas of the basal ganglia in macaques. Brain Res Bull 41:151–158.

Gerfen CR, Engber TM, Mahan LC, Susel Z, Chase TN, Monsma FJ, Sibley DR (1990) D1 and D2 dopamine receptor-regulated gene expression of striatonigral and striatopallidal neurons. Science 250:1429–1432.

Geurts M, Maloteaux JM, Hermans E (2003) Altered expression of regulators of G-protein signaling (RGS) mRNAs in the striatum of rats undergoing dopamine depletion. Biochem Pharmacol 66:1163–1170.

Glick JL, Meigs TE, Miron A, Casey PJ (1998) RGSZ1, a Gz-selective regulator of G protein signaling whose action is sensitive to the phosphorylation state of Gzalpha. J Biol Chem 273:26008–26013.

Gold SJ, Ni YG, Dohlman HG, Nestler EJ (1997) Regulators of G-protein

signaling (RGS) proteins: region-specific expression of nine subtypes in rat brain. J Neurosci 17:8024–8037.

Gold SJ, Han MH, Herman AE, Ni YG, Pudiak CM, Aghajanian GK, Liu RJ, Potts BW, Mumby SM, Nestler EJ (2003) Regulation of RGS proteins by chronic morphine in rat locus coeruleus. Eur J Neurosci 17:971–980.

Grafstein-Dunn E, Young KH, Cockett MI, Khawaja XZ (2001) Regional distribution of regulators of G-protein signaling (RGS) 1, 2, 13, 14, 16, and GAIP messenger ribonucleic acids by in situ hybridization in rat brain. Brain Res Mol Brain Res 88:113–123.

Granneman JG, Zhai Y, Zhu Z, Bannon MJ, Burchett SA, Schmidt CJ, Andrade R, Cooper J (1998) Molecular characterization of human and rat RGS 9L, a novel splice variant enriched in dopamine target regions, and chromosomal localization of the RGS 9 gene. Mol Pharmacol 54:687–694.

Guigoni C, Dovero S, Aubert I, Li Q, Bioulac BH, Bloch B, Gurevich EV, Gross CE, Bezard E (2005a) Levodopa-induced dyskinesia in MPTP-treated macaques is not dependent on the extent and pattern of nigrostrial lesioning. Eur J Neurosci 22:283–287.

Guigoni C, Li Q, Aubert I, Dovero S, Bioulac BH, Bloch B, Crossman AR, Gross CE, Bezard E (2005b) Involvement of sensorimotor, limbic, and associative basal ganglia domains in L-3,4-dihydroxyphenylalanine-induced dyskinesia. J Neurosci 25:2102–2107.

He W, Cowan CW, Wensel TG (1998) RGS9, a GTPase accelerator for phototransduction. Neuron 20:95–102.

Huot P, Levesque M, Parent A (2007) The fate of striatal dopaminergic neurons in Parkinson's disease and Huntington's chorea. Brain 130:222–232.

Kovoor A, Seyffarth P, Ebert J, Barghshoon S, Chen CK, Schwarz S, Axelrod JD, Cheyette BN, Simon MI, Lester HA, Schwarz J (2005) D_2 dopamine receptors colocalize regulator of G-protein signaling 9–2 (RGS9–2) via the RGS9 DEP domain, and RGS9 knock-out mice develop dyskinesias associated with dopamine pathways. J Neurosci 25:2157–2165.

Krumins AM, Barker SA, Huang C, Sunahara RK, Yu K, Wilkie TM, Gold SJ, Mumby SM (2004) Differentially regulated expression of endogenous RGS4 and RGS7. J Biol Chem 279:2593–2599.

Linder ME, Middleton P, Hepler JR, Taussig R, Gilman AG, Mumby SM (1993) Lipid modifications of G proteins: alpha subunits are palmitoylated. Proc Natl Acad Sci USA 90:3675–3679.

Lindskog M, Svenningsson P, Fredholm B, Greengard P, Fisone G (1999) Mu- and delta-opioid receptor agonists inhibit DARPP-32 phosphorylation in distinct populations of striatal projection neurons. Eur J Neurosci 11:2182–2186.

Lundblad M, Andersson M, Winkler C, Kirik D, Wierup N, Cenci MA (2002) Pharmacological validation of behavioural measures of akinesia and dyskinesia in a rat model of Parkinson's disease. Eur J Neurosci 15:120–132.

Lundblad M, Picconi B, Lindgren H, Cenci MA (2004) A model of L-DOPA-induced dyskinesia in 6-hydroxydopamine lesioned mice: relation to motor and cellular parameters of nigrostriatal function. Neurobiol Dis 16:110–123.

MacKenzie RG, Stachowiak MK, Zigmond MJ (1989) Dopaminergic inhibition of striatal acetylcholine release after 6-hydroxydopamine. Eur J Pharmacol 168:43–52.

Mallet N, Le Moine C, Charpier S, Gonon F (2005) Feedforward inhibition of projection neurons by fast-spiking GABA interneurons in the rat striatum *in vivo*. J Neurosci 25:3857–3869.

Meissner W, Ravenscroft P, Reese R, Harnack D, Morgenstern R, Kupsch A, Klitgaard H, Bioulac B, Gross CE, Bezard E, Boraud T (2006) Increased slow oscillatory activity in substantia nigra pars reticulata triggers abnormal involuntary movements in the 6-OHDA-lesioned rat in the presence of excessive extracellular striatal dopamine. Neurobiol Dis 22:586–598.

Nadjar A, Brotchie JM, Guigoni C, Li Q, Zhou SB, Wang GJ, Ravenscroft P, Georges F, Crossman AR, Bezard E (2006) Phenotype of striatofugal medium spiny neurons in parkinsonian and dyskinetic nonhuman primates: a call for a reappraisal of the functional organization of the basal ganglia. J Neurosci 26:8653–8661.

Paxinos G, Watson C (1986) The rat brain in stereotaxic coordinates, Ed 1. San Diego: Academic.

Picconi B, Centonze D, Hakansson K, Bernardi G, Greengard P, Fisone G, Cenci MA, Calabresi P (2003) Loss of bidirectional striatal synaptic plasticity in L-DOPA-induced dyskinesia. Nat Neurosci 6:501–506.

Psifogeorgou K, Papakosta P, Russo SJ, Neve RL, Kardassis D, Gold SJ, Zachariou V (2007) RGS9–2 is a negative modulator of mu-opioid receptor function. J Neurochem 103:617–625.

Rahman Z, Gold SJ, Potenza MN, Cowan CW, Ni YG, He W, Wensel TG, Nestler EJ (1999) Cloning and characterization of RGS9–2: a striatal-enriched alternatively spliced product of the RGS9 gene. J Neurosci 19:2016–2026.

Rahman Z, Schwarz J, Gold SJ, Zachariou V, Wein MN, Choi KH, Kovoor A, Chen CK, DiLeone RJ, Schwarz SC, Selley DE, Sim-Selley LJ, Barrot M, Luedtke RR, Self D, Neve RL, Lester HA, Simon MI, Nestler EJ (2003) RGS9 modulates dopamine signaling in the basal ganglia. Neuron 38:941–952.

Rascol O, Brooks DJ, Korczyn AD, De Deyn PP, Clarke CE, Lang AE (2000) A five-year study of the incidence of dyskinesia in patients with early Parkinson's disease who were treated with ropinirole or levodopa. 056 Study Group. N Engl J Med 342:1484–1491.

Ross EM, Wilkie TM (2000) GTPase-activating proteins for heterotrimeric G proteins: regulators of G protein signaling (RGS) and RGS-like proteins. Annu Rev Biochem 69:795–827.

Taymans JM, Kia HK, Claes R, Cruz C, Leysen J, Langlois X (2004) Dopamine receptor-mediated regulation of RGS2 and RGS4 mRNA differentially depends on ascending dopamine projections and time. Eur J Neurosci 19:2249–2260.

Tekumalla PK, Calon F, Rahman Z, Birdi S, Rajput AH, Hornykiewicz O, Di Paolo T, Bedard PJ, Nestler EJ (2001) Elevated levels of DeltaFosB and RGS9 in striatum in Parkinson's disease. Biol Psychiatry 50:813–816.

Waugh JL, Lou AC, Eisch AJ, Monteggia LM, Muly EC, Gold SJ (2005) Regional, cellular, and subcellular localization of RGS10 in rodent brain. J Comp Neurol 481:299–313.

Zachariou V, Georgescu D, Sanchez N, Rahman Z, DiLeone R, Berton O, Neve RL, Sim-Selley LJ, Selley DE, Gold SJ, Nestler EJ (2003) Essential role for RGS9 in opiate action. Proc Natl Acad Sci USA 100:13656–13661.

Zhang S, Coso OA, Lee C, Gutkind JS, Simonds WF (1996) Selective activation of effector pathways by brain-specific G protein beta5. J Biol Chem 271:33575–33579.